SYNTHESIS OF GOLD NANOPARTICLES FOR CANCER THERAPEUTIC APPLICATIONS

A Thesis
Presented to
The Academic Faculty

by

Ant Yucesoy

In Partial Fulfillment
Of the Requirements for the Degree
B.S. in Biomedical Engineering in the
Department of Biomedical Engineering

Georgia Institute of Technology
December 2014

SYNTHESIS OF GOLD NANOPARTICLES FOR CANCER THERAPEUTIC APPLICATIONS

Approved by:

Dr. Younan Xia, Advisor
School of Biomedical Engineering and Chemistry
Georgia Institute of Technology

Dr. Manu O. Platt
School of Biomedical Engineering
Georgia Institute of Technology

Dr. Ravi Bellamkonda
School of Biomedical Engineering
Georgia Institute of Technology

Date Approved: December 12, 2014

ACKNOWLEDGEMENTS

I would like to begin by thanking my mother and father, without whom I would not exist in this realm. I would also like to thank them for their guidance and support. I also wish to thank my principal investigator Dr. Younan Xia for giving me the opportunity to work two long and productive years in his world renowned nanotechnology lab and for letting me participate in his groundbreaking research. In addition, I would like to thank the mentors I had to teach me along the way: Dr. Yucai Wang, Dr. Tianmeng Sun, and Bo Pang.

TABLE OF CONTENTS

LIST OF TABLES

LIST OF FIGURES

LIST OF SYMBOLS AND ABBREVIATIONS

Au	Gold
AgNC	Silver Nanocubes
AuNC	Gold Nanocages
AuNR	Gold Nanorods
AuNS	Gold Nanospheres
CSC	Cancer Stem Cells
ICP-MS	Inductively Coupled Plasma Mass Spectrometry
TEM	Transmission Electron Microscopy

SUMMARY

Gold (Au) nanostructures have received considerable attention in recent years due to their advantageous chemical and physical properties and potential applications in cancer diagnosis and treatment. Easily controllable size, geometry, and nontoxicity of Au nanostructures enable their diverse array of biomedical applications.

Cancer stem cells (CSCs) are subpopulations of cells within tumors that drive tumor growth, metastasis and recurrence. CSCs are resistant to many current cancer treatments, including chemo and radiation therapy. As these cells are both invasive and highly tumorigenic, it has been hypothesized that the inability to efficiently eliminate CSCs during conventional therapy may result in disease relapse and formation of metastases. Recent studies have described new treatment modalities to deliver therapeutic payloads directly to CSCs using nanoparticles.

Despite the successful use of Au nanoparticles for cancer therapy both in vitro and in vivo, their CSC targeting capability remain largely unexplored. The objective of this project is to investigate the significance of shape, size, and culture time in the distribution of Au nanoparticles in CSCs and non-CSCs and to understand the underlying mechanisms of internalization.

CHAPTER 1

INTRODUCTION

Cancer Stem Cell Persistence

Although they only constitute a small portion of a tumor, cancer stem cells (CSCs) are believed to be responsible for the origin, growth, recurrence, and metastasis of cancer. Current anticancer therapies (e.g., chemotherapy and radiation treatment) have been demonstrated to be ineffective against CSCs due to their indiscriminate cytotoxicity. More recently, studies have shown that conventional therapies enrich the CSC population due to their inherent resistance against these treatment regimes. This leads to high rates of tumor relapse and ultimate treatment failure (1). These limitations have provided incentives to develop effective anti-cancer strategies to target CSCs.

Gold Nanoparticles for Cancer Therapy

Nanoparticle-mediated delivery of chemotherapeutic agents has demonstrated enhanced anticancer efficacy while simultaneously reducing side effects of cancer treatment. Although nanoparticles with the proper structures, sizes, and surface properties have been shown to accumulate and retain in solid tumors, the importance of particle size and structure in this process remain largely unexplored.

We have chosen Au nanoparticles for initial studies due to their low cytotoxicity, size and shape controlled synthesis, uniformity, and well-developed surface chemistry. Current studies have demonstrated the use of Au nanoparticles for a wide range of biomedical applications, including RNA interference therapy and programmed

cell death (2, 3). Recently, Xia and Li (4) reported theranostic applications of Au nanoparticles in photoacoustic imaging and as a photothermal agent and drug delivery vehicle.

Previous research has already shown that cellular uptake of Au nanoparticles depends on their particular shape, size, and surface ligands (5-7). Nanoparticles with the proper structure and size readily accumulate and retain in solid tumors. However, it is still not clear whether the size and shape characteristics of Au nanoparticles influence their uptake by CSCs (8). In addition, comparative uptake of different Au nanostructures (spherical, cubic and other shapes) by CSCs has not been investigated. In this study, we aimed to investigate the size and shape dependence of Au nanoparticle uptake into CSCs and non-CSCs. The results of this research may help optimize maximal biodistribution of the particles for an increased anti-tumor capability.

Research Objective

The objective of this study is to characterize the biodistribution of Au nanoparticles in CSCs and non-CSCs. In order to compare the cellular internalization of nanoparticles with different shape and size and understand the related mechanism of internalization, Au nanoparticles with varying 3-D shape and size will be synthesized. Figure 1 shows transmission electron microscopy (TEM) images of Au nanospheres, Au nanocages and Au nanorods. The aqueous suspensions of these nanoparticles will be incubated with CSCs and non-CSCs and the amount of particles inside these cells will be analyzed using inductively coupled plasma mass spectrometry (ICP-MS).

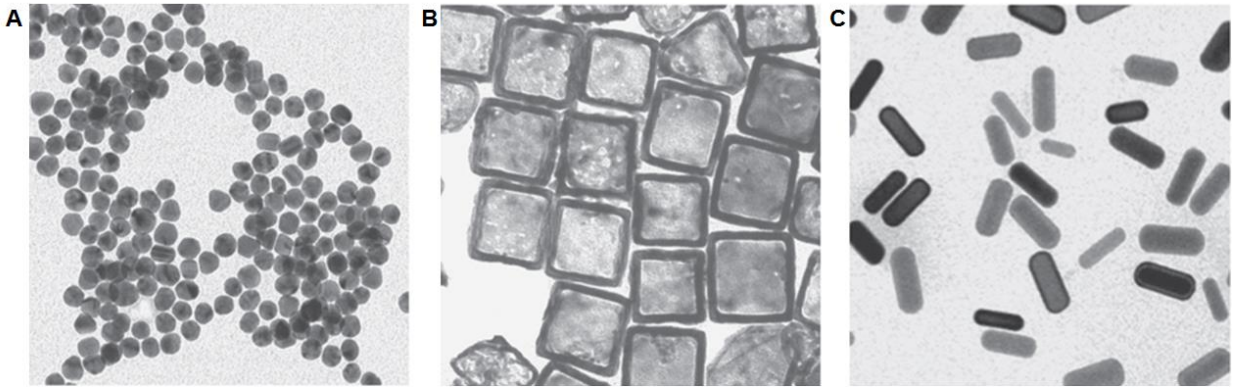

Figure 1: The Transmission Electron Microscopy (TEM) Images of Different Nanoparticles: (a) Au nanospheres, (b) Au nanocages and (c) Au nanorods.

In the first stage of this project, 20, 50, and 100 nm au nanospheres were synthesized. Figure 2 shows TEM images of Au nanospheres with different sizes. The Au nanoparticles were then conjugated with polyethylene glycol (PEG) to prevent agglomeration by interaction with plasma proteins during the culture (9). MDA-MB-435 cells derived from mice breast cancer tissue were cultured in serum-free DMEM-F12 medium that contained a supplement of nutrients, growth factors and hormones. This culture condition induced the cancer cells to form mammospheres (spherical collection of cells) and enriched the CSCs from about 5% to 50%. The mammosphere cells were incubated in Au nanoparticle solutions for varying lengths of culture time. these cells were then labeled with ALDH1 (a marker for breast CSCs) and CSCs were isolated by fluorescence activated cell sorter.

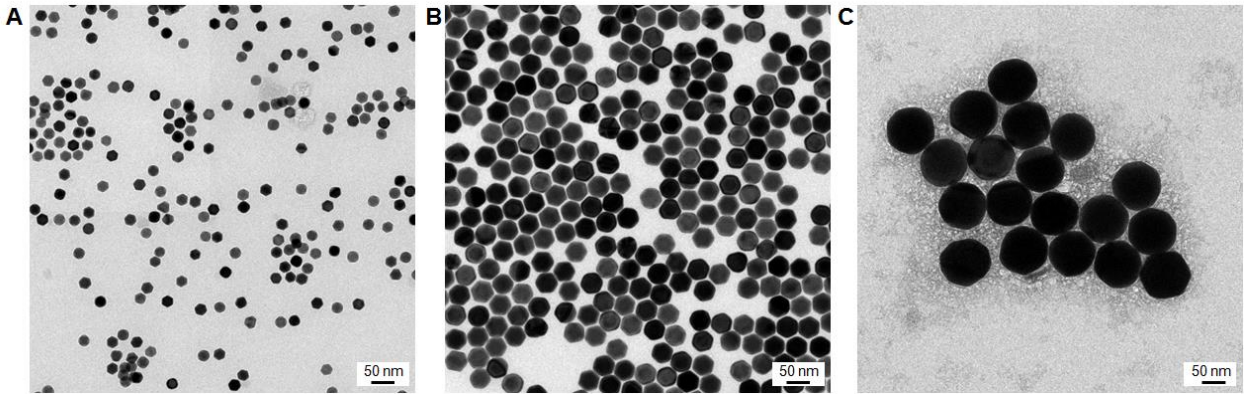

Figure 2: The Transmission Electron Microscopy (TEM) Images of Au Nanospheres with Different Sizes: (a) 20 nm, (b) 50 nm and (c) 100 nm**.**

CHAPTER 2

MATERIALS AND METHODS

Materials

Hexadecyltrimethylammonium bromide (CTAB, >98.0%), hexadecyltrimethylammonium chloride (CTAC, >98.0%), MeOH, 5-bromosalicylic acid (5-BrSA, >98.0%), hydrogen tetrachloroaurate trihydrate ($HAuCl_4 \cdot 3H_2O$), sodium salicylate (NaCreso, 99%), L-ascorbic acid (>99.5%), silver nitrate ($AgNO_3$, >99%), sodium borohydride ($NaBH_4$, 99%), hydrochloric acid (HCl, 37 wt% in water), silver trifluoroacetate (CF_3COOAg, >98%), sodium hydrosulfide hydrate (NaHS) and polyvinylpyrrolidone (PVP, MW≈55,000) were purchased from sigma aldrich. Sodium chloride (NaCl, 99.9%) was acquired from Fisher, Fairlawn, NJ. *Trans*-2-[3-(4-tert-butylphenyl)-2-methyl-2-propenylidene] malononitrile (DCTB) was obtained from Santa Cruz Biotechnology and used as received. Ethylene glycol (EG) was acquired from J. T. Baker (lot no. G32B27). Methoxy-terminated PEG-thiol (1 mM, mPEG-SH) was purchased from Laysan Bio. Inc. DMEM-F12 media and supplements

were purchased from Invitrogen. Ultrapure water with a resistivity of 18.2 MΩcm produced with Milli-Q Integral 5 system was used in all experiments. All glassware was rinsed extensively with ultrapure water and dried before use.

Synthesis of Gold Nanorods

The seed solution for AuNRs was prepared as follows (10, 11): A 5 mL amount of 0.5 mM $HAuCl_4$ was mixed with 5 mL of 0.2 M CTAB solution. A 0.6 mL portion of fresh 0.01 M NaBH4 was then quickly injected into the Au (III)-CTAB solution without stirring. The solution color changed from yellow to brownish-yellow. The seed solution was aged at room temperature for 30 min before use.

To prepare the growth solution, 0.9 g of CTAB together with defined amounts of additives were dissolved in 25 mL of warm water (60^{o}C) in a 100 mL round flask. The solution was allowed to cool to 30^{o}C after a 4 mM $AgNO_3$ solution was added. The mixture was kept undisturbed at 30^{o}C for 15 min, after which 25 mL of 1 mM HAuCl4 solution and, if necessary, a small amount of HCl (37 wt% in water, 12.1 M) was added. After 15 min of slow stirring (400 rpm), 0.064 M ascorbic acid (Table 1) was added, and the solution was vigorously stirred for 30 s until it became colorless. The growth solution had a CTAB concentration of about 0.05 M and was used right after preparation. Table 1 shows the required amounts of each chemical for different sizes of nanorods.

Finally, 0.08 mL of seed solution was injected into the growth solution. The resultant mixture was stirred for 30 s and left undisturbed at 30^{o}C for 12 h for nanorod growth. The reaction products were isolated by centrifugation at 8,500 rpm for 25

min followed by removal of the supernatant. The precipitates were redispersed in 10 mL of water.

Additive	Seed Solution (mL)	$AgNO_3$ (mL)	Ascorbic Acid (mL)	Dimensions (nm)	LSPR from FDTD calculation (nm)
Na-creso, 0.11 g	0.08	0.60	0.10	Length:33.0 ± 2.5 Diamtr:14.0 ± 1.0	630
5-BrSA, 0.11 g	0.08	2.40	0.20	49.0 ± 4.0 10.0 ± 1.0	886
5-BrSA, 0.11 g	0.04	1.80	0.20	52.5 ± 3.5 12.0 ± 0.5	828
0.11g 5-BrSA + 0.21 mL HCl	0.04	2.40	0.125	101.7 ± 7.5 15.9 ± 0.8	1057

Table 1: Reagent Requirements Table: Shows the required amounts of each chemical for different sizes of nanorods.

Synthesis of Gold Nanospheres

Preparation of the initial CTAB-Capped Au Seeds was as follows (12): The Au seeds were prepared by adding an ice-cold aqueous solution of $NaBH_4$ (0.6 mL, 10 mM) into an aqueous solution of $HAuCl_4$ (10 mL, 0.25 mM) and CTAB (100 mM). A brown solution immediately formed upon the introduction of $NaBH_4$. Then, the mixture was left undisturbed at 27^oC for 3 h to ensure the complete decomposition of any $NaBH_4$ that remained in the reaction mixture.

In a standard synthesis of 10 nm Au nanospheres, an aqueous solution of $HAuCl_4$ (2 mL, 0.5 mM), an aqueous solution of CTAC (2 mL, 200 mM), and an aqueous solution of AA (1.5 mL, 100 mM) were mixed in a glass vial (20 mL), followed by the addition of the initial seeds (100 mL). The reaction was allowed to proceed at 27^oC for 10 min.

The product was collected by centrifugation at 14,500 rpm for 30 min and washed once with water.

For the synthesis of 20 nm Au nanospheres, an aqueous solution of $HAuCl_4$ (2 mL, 0.25 mM), an aqueous solution of CTAC (2 mL, 200 mM), and an aqueous solution of AA (1.5 mL, 50 mM) were mixed in a vial (20 mL), followed by the addition of the as-prepared suspension of 10 nM Au nanospheres (100 mL, before washing). The reaction was allowed to proceed at 27°C for 10 min. The final product was collected by centrifugation at 14,500 rpm for 10 min and washed once with water. Protocol for 50 and 100 nm nanospheres has recently been submitted (13).

Synthesis of Gold Nanocages

Preparation of Silver Nanocubes.

Single-crystal seeds of Ag were prepared using a recently reported polyol process (14-16) with ethylene glycol (EG) as the solvent and CF_3COOAg as a precursor to elemental silver. In a typical synthesis, 5 mL EG was added into a 100 mL round bottom flask and heated under magnetic stirring in an oil bath pre-set to 150 °C, and then 0.06 mL NaHS (3 mM in EG) was quickly injected. After 2 min, 0.5 mL HCl (3 mM in EG) was injected into the heated solution, followed by the addition of 1.25 mL of poly (vinyl pyrrolidone) (20 mg/mL in EG). After another 2 min, 0.4 mL CF_3COOAg (282 mM in EG) was added into the mixture. During the entire process, the flask was capped with a glass stopper except the addition of reagents. The cubic seeds were obtained by quenching the reaction with an ice-water bath when the major LSPR peak of the Ag seeds had reached 399 nm and 435 nm, respectively. After centrifugation and

washing with acetone and deionized water three times, the seeds were stored in EG. The particle concentration of Ag seeds was determined using a combination of TEM imaging (for size measurement) and ICP-MS, for the Ag concentration.

Titration of Silver Nanostructures with $HAuCl_4$ Solution.

In a typical procedure (17, 18), a 100 µl aliquot of the as-obtained dispersion of silver nanocubes (or 250 µl for the nanowires or spherical nanoparticles) was added to 5 ml of deionized water. This diluted dispersion of silver nanocubes was then refluxed for 10 min before a specific volume of 1 mm $HAuCl_4$ aqueous solution was added dropwise. The mixture was refluxed for another 20 min until its color became stable. Vigorous magnetic stirring was maintained in the entire process. As the solution was cooled to room temperature, white solids AgCl precipitates was found to settle at the bottom of the container. The AgCl solid could be removed by dissolving with a saturated solution of NaCl. In this case, NaCl powders were added to the aqueous dispersion of product until it was saturated with NaCl. The solution was then transferred into a tube and centrifuged at 10,000 rpm for 15 min. The supernatant containing the dissolved AgCl could be easily removed using a pipe. The solid was rinsed with water and centrifuged six more times and finally dispersed with water for further characterization and usage.

PEGylation

The PEG-modification was prepared by adding 0.3 mL of 1 mM mPEG-SH (Laysan Bio Inc., Arab, AL) to 1 mL of the as-prepared or as obtained Au nanoparticles

at room temperature. After 12 h, the PEG-modified Au nanoparticles were separated by centrifugation and redispersed in deionized water.

Internalization

MDA-MB-435 breast cancer stem cells were enriched in serum-free DMEMF12 media with growth factors. Figure 3 shows images of adherent cells and mammospheres of MDA-MB-435 cells. The mammosphere cells were treated with Au nanospheres with different sizes for various culture times. The CSCs and non-CSCs in mammospheres were separately collected using BD Biosciences FACS Aria III cell sorter. The number of Au nanoparticles taken up by the cells was then quantified using ICP-MS for both CSCs and non-CSCs.

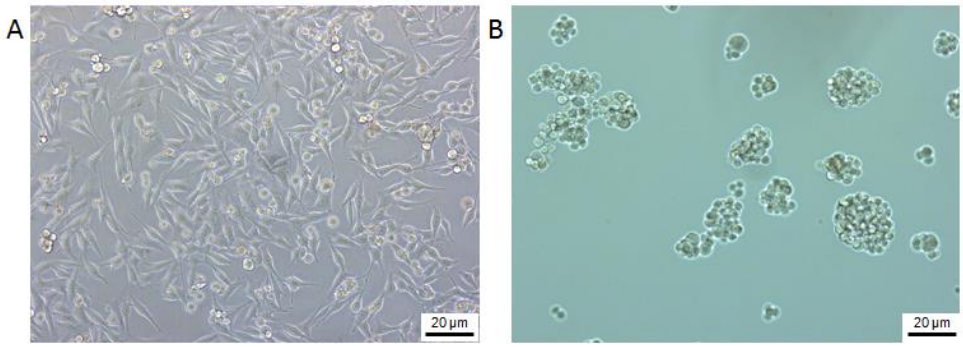

Figure 3: The Bright-Field Images of Cells: (a) adherent cells and (b) mammospheres of MDA-MB-435 cells.

CHAPTER 3

RESULTS

In this stage of the project, we tested only nanospheres of different sizes (20, 50, and 100 nm) in MDA-MB-435 CSCs and non-CSCs. We found that the internalization of Au

nanospheres is time and size-dependent in both CSCs and non-CSCs. Higher internalization efficiency is defined as having higher distribution of particles within CSCs than non-CSCs.

Although the highest internalization efficiency was achieved at 6 h incubation period with 20 nm nanospheres, internalization efficiency was also higher at other time points assessed (0.5, 1, 2, and 4 h) as compared to 50 and 100 nm nanostructures. Figure 4 shows internalization efficiency of tested Au nanospheres.

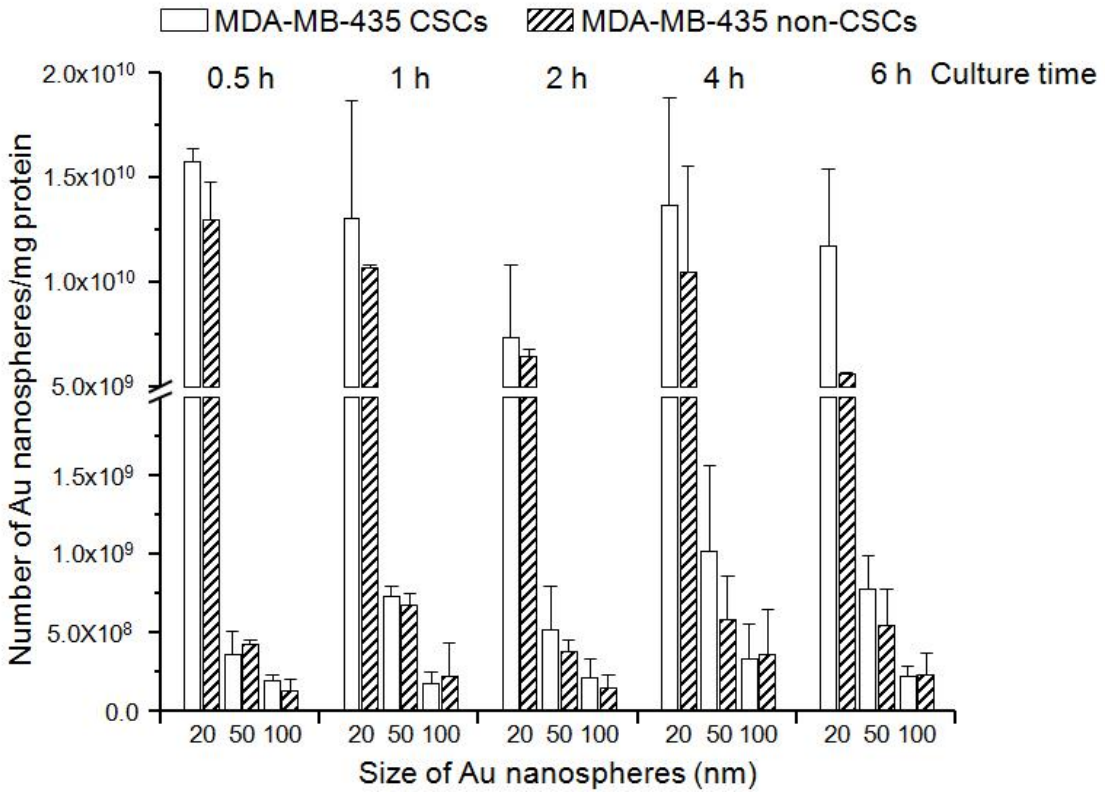

Figure 4: **The Internalization Efficiency of Au Nanospheres with Different Sizes by CSCs and non-CSCs in Vitro.** The amount of nanospheres in the cells was determined by ICP-MS analysis. Highest internalization efficiency was achieved at 6 h incubation period with 20 nm nanospheres. Error bars represent standard deviation.

CHAPTER 3

DISCUSSION

Nanoparticles are increasingly used in biomedical applications ranging from drug delivery to cellular imaging (4, 18). Their size and shape have been shown to be important in their CSC targeting capacity. In this preliminary work, we investigated size and time-dependent cellular internalization of Au nanospheres into CSCs. Our results showed that cellular uptake of Au nanospheres by CSCs is size and time-dependent. Although internalization rate of all sizes of Au nanospheres in CSCs were higher than that observed for non-CSCs at all time points assessed, the highest internalization efficiency was observed at 6 h with 20 nm Au nanospheres. This shows that longer contact and smaller size of Au nanospheres are important for an increased CSC internalization efficiency. The internalization process by cells (both CSCs and non-CSCs) is mostly like through the process of endocytosis. We will repeat these experiments for the consistency of results. It is highly possible that presence of different Au nanoparticles in the medium could affect the cellular uptake of each other. Also, in these applications, nanoparticles are exposed to a complex cellular environment and this may alter nanoparticle–cell interactions (8). Therefore, a large number of in vitro experiments need to be conducted to compare differential internalization of nanostructures with different sizes and shapes alone or in combination and interaction of nanoparticles with extracellular proteins should be taken into consideration. Once internalization rate and pattern of different Au

nanostructures are identified, in vivo experiment will be designed to test tumor targeting capacity of these nanostructures in tumor bearing mice.

REFERENCES

1. Zhou BB, Zhang H, Damelin M, Geles KG, Grindley JC, Dirks PB. Tumour-initiating cells: challenges and opportunities for anticancer drug discovery. Nature reviews Drug discovery. 2009;8(10):806-23. Epub 2009/10/02.

2. Doss CG, Debajyoti C, Debottam S. Disruption of Mitochondrial Complexes in Cancer Stem Cells Through Nano-based Drug Delivery: A Promising Mitochondrial Medicine. Cell Biochem Biophys. 2013:1-5.

3. Song WJ, Du JZ, Sun TM, Zhang PZ, Wang J. Gold nanoparticles capped with polyethyleneimine for enhanced siRNA delivery. Small. 2010;6(2):239-46. Epub 2009/11/20.

4. Xia Y, Li W, Cobley CM, Chen J, Xia X, Zhang Q, et al. Gold nanocages: from synthesis to theranostic applications. Accounts of chemical research. 2011;44(10):914-24. Epub 2011/05/03.

5. Cho EC, Au L, Zhang Q, Xia Y. The effects of size, shape, and surface functional group of gold nanostructures on their adsorption and internalization by cells. Small. 2010;6(4):517-22. Epub 2009/12/24.

6. Cho EC, Liu Y, Xia Y. A simple spectroscopic method for differentiating cellular uptakes of gold nanospheres and nanorods from their mixtures. Angew Chem Int Ed Engl. 2010;49(11):1976-80. Epub 2010/02/11.

7. Zhang Y, Tekobo S, Tu Y, Zhou Q, Jin X, Dergunov SA, et al. Permission to Enter Cell by Shape: Nanodisk vs Nanosphere. ACS applied materials & interfaces. 2012;4(8):4099-105. Epub 2012/07/31.

8. Cho EC, Zhang Q, Xia Y. The effect of sedimentation and diffusion on cellular uptake of gold nanoparticles. Nature nanotechnology. 2011;6(6):385-91. Epub 2011/04/26.

9. Qian W, Murakami, M., Ichikawa, Y., & Che, Y. . Highly Efficient and Controllable PEGylation of Gold Nanoparticles Prepared by Femtosecond Laser Ablation in Water. The Journal of Physical Chemistry C. 2011;115(47):23293-8.

10. Ye X, Jin L, Caglayan H, Chen J, Xing G, Zheng C, et al. Improved size-tunable synthesis of monodisperse gold nanorods through the use of aromatic additives. ACS nano. 2012;6(3):2804-17. Epub 2012/03/02.

11. Ye X, Zheng C, Chen J, Gao Y, Murray CB. Using Binary Surfactant Mixtures To Simultaneously Improve the Dimensional Tunability and Monodispersity in the Seeded Growth of Gold Nanorods. Nano Letters. 2013;13(2):765-71.

12. Zheng Y, Ma Y, Zeng J, Zhong X, Jin M, Li ZY, et al. Seed-mediated synthesis of single-crystal gold nanospheres with controlled diameters in the range 5-30 nm and their self-assembly upon dilution. Chemistry, an Asian journal. 2013;8(4):792-9. Epub 2013/01/31.

13. Y. Zheng YX. Part. Part. Syst. Charact. 2013.

14. Wang Y, Zheng Y, Huang CZ, Xia Y. Synthesis of Ag Nanocubes 18-32 nm in Edge Length: The Effects of Polyol on Reduction Kinetics, Size Control, and Reproducibility. Journal of the American Chemical Society. 2013;135(5):1941-51. Epub 2013/01/16.

15. Zhang Q, Li W, Moran C, Zeng J, Chen J, Wen LP, et al. Seed-mediated synthesis of Ag nanocubes with controllable edge lengths in the range of 30-200 nm and comparison of their optical properties. Journal of the American Chemical Society. 2010;132(32):11372-8. Epub 2010/08/12.

16. Zhang Q, Li W, Wen LP, Chen J, Xia Y. Facile synthesis of Ag nanocubes of 30 to 70 nm in edge length with CF(3)COOAg as a precursor. Chemistry. 2010;16(33):10234-9. Epub 2010/07/02.

17. Chen J, McLellan JM, Siekkinen A, Xiong Y, Li ZY, Xia Y. Facile synthesis of gold-silver nanocages with controllable pores on the surface. Journal of the American Chemical Society. 2006;128(46):14776-7. Epub 2006/11/16. 11

18. Wang Y, Liu Y, Luehmann H, Xia X, Brown P, Jarreau C, et al. Evaluating the pharmacokinetics and in vivo cancer targeting capability of au nanocages by positron emission tomography imaging. ACS nano. 2012;6(7):5880-8. Epub 2012/06/14.